ANWENDUNG DIGITALER VERARBEITUNG VON TEILENTLADUNGEN FÜR DIE DIAGNOSE UND MONITORING VON HOCHSPANNUNGSKOMPONENTEN

Edward Gulski
Technische Universität Delft, Hochspannungslaboratorium
Mekelweg 4, 2628 CD Delft, Niederlande

1. Introduction

HV equipment is usually tested for discharges using conventional discharge detection (bandwidths up to hundreds of kHz). Due to the increasing automatization of PD measurements in recent years, the use of digital evaluation has become very popular. It's known that the digital recording of measuring information permits a more systematic analysis of the discharge process [1].
Practical implications of new *fingerprint* technique as used in a commercialized method (TEAS) will be presented here and will be discussed in the scope of the following goals [2].
The main goal of the automatization is to create additional information about the source of the discharge. As a result, the electrical engineer will be aided in his decision about conditions of an insulating construction. In particular, **the manufacturer** of HV constructions is interested in controlling the quality of his product, **the testing institution** is interested to certify the product and finally **the user** of HV construction is interested to know the residual life of his equipment.

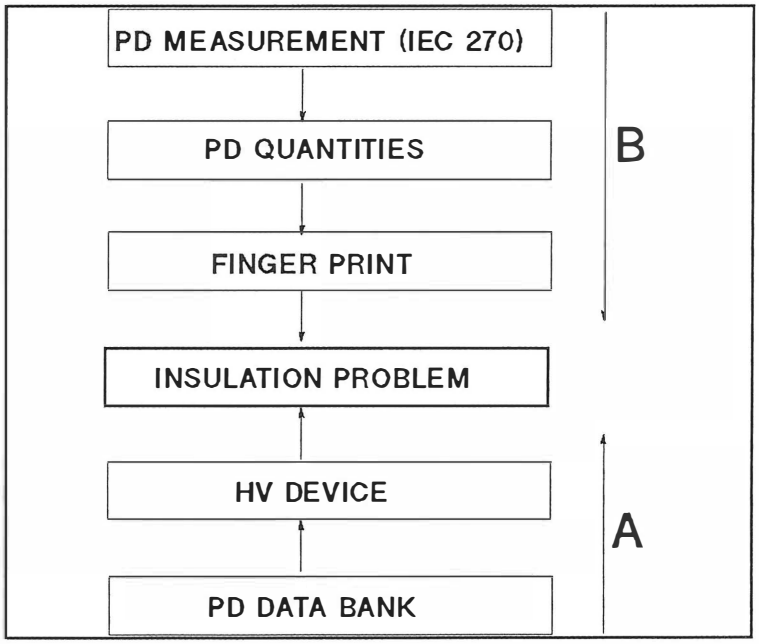

Figure 1 The structure of a PD data bank. First a category of the data bank is selected which corresponds with the objectives of the user (arrow A), then a number of measurements which belong to this category will be combined into problems (arrow B).

Thus, there is a need to develop **techniques** to analyze the discharges and to produce a ***PD data bank*** for such purposes as the **development**, the **manufacturing** or the **monitoring** of HV constructions, see figure 1.
When the information of a discharge pattern can be quantified, resulting in e.g. a ***fingerprint*** of the measurement, it can be used for comparison with unknown

situations [3]. In this way, most of specific design- or manufacturing-problems which may lead to discharge can be classified. As a result, a more efficient identification of discharge sources is possible, see section 4 and 5.
According to recent results, using continuous monitoring, also the degradation of the insulation at the discharge site may be assessed in this way [4], see section 6.
As a result of this systematic application the discrimination of discharges in full scale HV constructions becomes more realistic.

2. Finger Print Processing

It's known, for a long time recognition was performed by eye, studying PD patterns at the ellipse at an oscilloscope screen. Here the patterns are studied which occur in the 50Hz(60Hz) sine wave. Each discharge pulse at the ellipse reflects the physical process at the discharge site. In the past a strong relationship has been found between the shape of these patterns and the type of defect causing them.
Using digital processing the PD pulses are grouped with respect to their intensity and their phase-angle, see figures 2 and 3.
It is known that each discharge source with its geometry, location in insulation, dielectric properties and applied field is characterized by a specific sequence of discharges. Analysis of phase-position quantities and of the discharge and energy histograms is thus a good means of discriminating between different discharge sources. Generally two questions are important here:

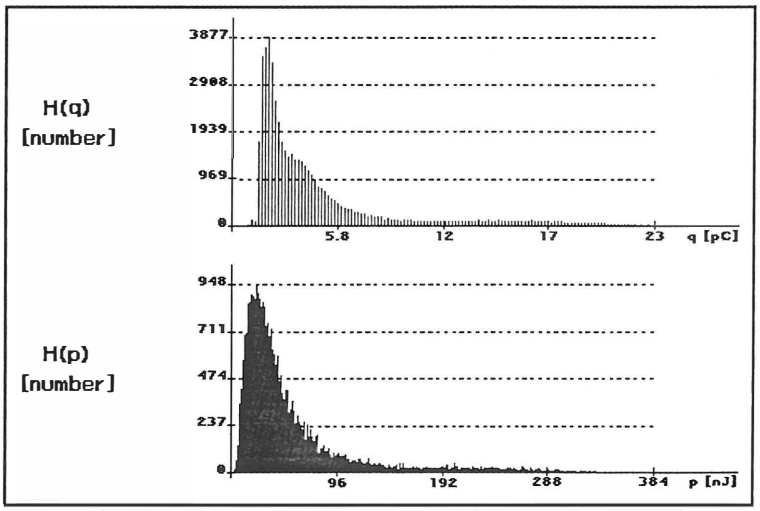

Figure 2 An example of discharge and energy distributions, which are processed to obtain the *Finger Print* of a PD measurement.

How to analyze and to quantify the information as contained in the envelopes of above mentioned distributions ? and
How to use these data to discriminate between different defects ?

To provide the analysis of all these distributions and above all to quantify their characteristic shapes *statistical operators* were introduced in the past [5].

1. The *asymmetry* of Hqn(ϕ), Hn(ϕ) and Hqmax(ϕ) as the quotient of the mean level in the (+) and in the (-).

2. The *phase factor* of Hqn(ϕ) to study the difference in inception voltage in the (+) and the (-).
3. The *cross-correlation* factor of Hqn(ϕ), Hn(ϕ) and Hqmax(ϕ) to evaluate the difference in shape between the (+) and the (-).
4. The *number of peaks* of Hqn±(ϕ), Hn±(ϕ) and Hqmax±(ϕ) to distinguish between a distribution with one single top and a distribution with several tops.

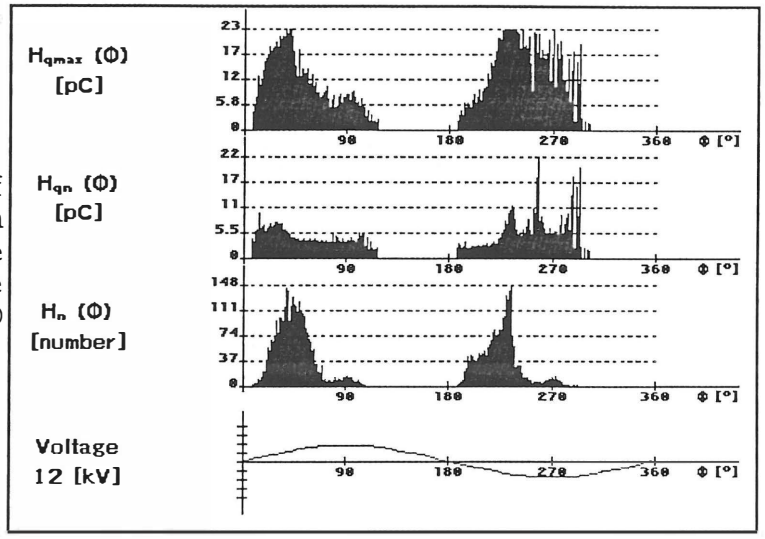

Figure 3 An example of phase-position quantities, which are processed to obtain the *Finger Print* of a PD measurement.

5. The *skewness* of Hqn±(ϕ), Hn±pm(ϕ), Hqmax±(ϕ), as an indicator for the asymmetry of a distribution with respect to a normal distribution.
6. The *kurtosis* of Hqn±(ϕ), Hn±(ϕ), Hqmax±(ϕ) as an indicator for the deviation from the normal distribution.

After a PD measurement has been finished, the above mentioned *statistical operators* are processed. Totally 29 statistical operators are processed to describe the properties of a PD measurement, see figure 4.

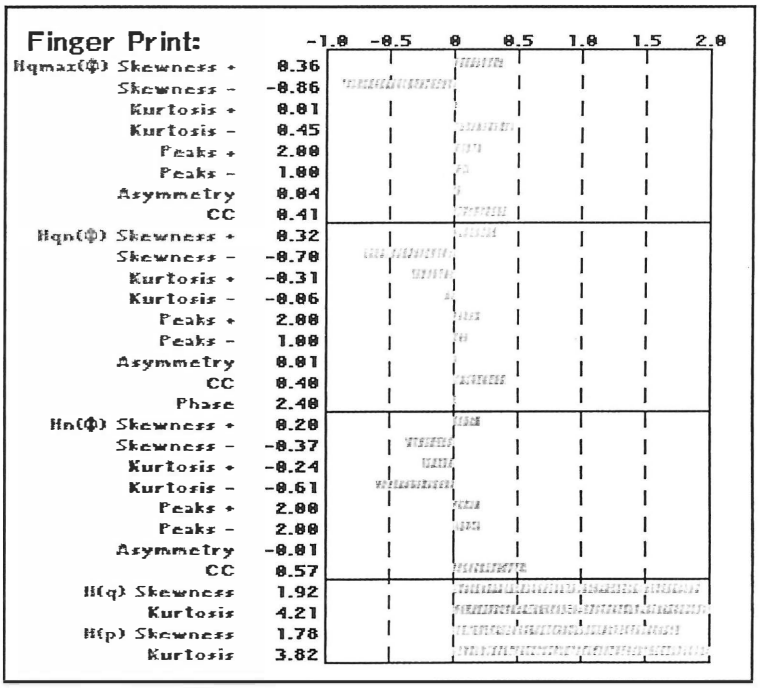

Figure 4 An example of a *Finger Print*.

Using such a *fingerprint* of a particular measurement a comparison with *fingerprints* of normalized PD sources like *cavity discharges, surface discharges, corona discharges* etc. is possible. For this purpose, using mathematical pattern recognition methods the percentage can be obtained which reflects the recognition of a particular measurement as a defined discharge type in the reference data [3].
In particular, for the number of *statistical operators* of reference data a collection of *fingerprint* occurs. The mathematical centre *C* of these *fingerprint* is determined and the position of an unknown discharge as represented by a set of *statistical operators X* can be compared with this centre. The recognition score is now defined as the percentile rank of the data (known fingerprint) which are further away from the centre *C* of the known discharge population than the measured value of an unknown discharge *X.* This percentage is not the same as the probability that *X* is indeed identical to the standard defect, but it gives the best possible reflection of it. The score of the unknown defect is 80% if eighty percent of the *fingerprint* of the reference data are further away from centre *C* than *X* itself.

3. Partial Discharge Data Bank

When several *fingerprints* are available, it is possible to develop a collection containing specific data: **the PD data bank**, see figure5. In this way an unknown discharge measurement as represented by its *fingerprint* can be compared to a collection of known situations.

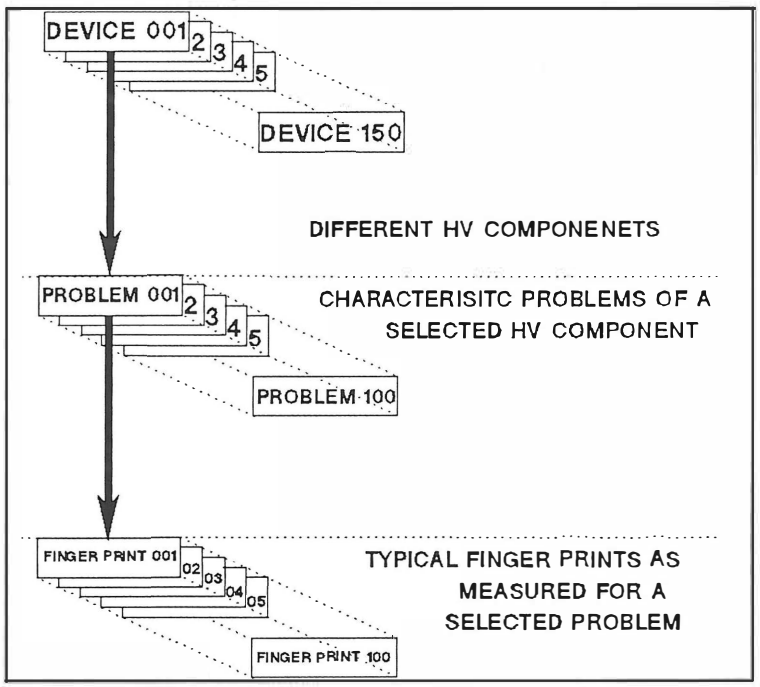

Figure 5 Structure of a PD Data Bank.

A data bank is judged to be well designed if it produces a high similarity for the correct defect and low or nil for all the others. If no recognition is possible, the result should be low or of nil similarity for all defects.
Of course, the result of such a recognition process strongly depends on the following factors: the test conditions at which the reference data are obtained,

the number of measurements used to represent a defect and the way the data bank is organized.
From a practical point of view it is attractive to organize such a data bank using a structure with three levels of storage:

device level: here each **device** represents one of different groups of PD sources, for instance 'ARTIFICIAL DEFECTS', 'EPOXY INSULATED CURRENT TRANSFORMER', 'PAPER/OIL BUSHING, 'GIS', etc.

problem level: each of above mentioned **devices** is characterized by means of specific **problems**, for instance the **device** 'ARTIFICIAL DEFECTS' contains *cavity discharges, surface discharges, corona discharges* etc.. An other **device** for instance 'GIS' may contain **problems** which may occur in the case of GIS construction only.

fingerprint level: each of the above mentioned problems is characterized by series of typical measurements.

This structure provides universal application of such a *PD data bank*. In the following two possible solution are discussed.

4. PD Source Recognition Using 'ARTIFICIAL DEFECTS'

The *device* called 'ARTIFICIAL DEFECTS' contains 17 *problems*: these problems are simple two-electrode models, representing 17 possible defects in the insulation [1,5]. In the following PD sources, their model description as well as the test conditions are listed which were used for analysis of discharges in HV components.

1. *Single corona discharges at the HV electrode in air;* diameter of high voltage point: 100um; distance to LV electrode: 30mm; test voltage: 2.2 kVeff.
2. *Single corona discharges at the LV electrode in air;* diameter of the low voltage point: 100 um; distance to HV electrode: 30 mm; test voltage: 2.3 kVeff.
3. *Surface PD between external LV electrode and PE surface;* LV cylinder-to-PE plane system; dielectric: polyethylene; LV electrode diameter: 20mm; average field strength: 2.8 kV/mm.
4. *Surface PD between external HV electrode and PE surface;* HV cylinder to-PE-plane system; dielectric: polyethylene; HV electrode diameter: 20 mm; average field strength: 3.4 kV/mm.
5. *Multiple corona discharges at the HV electrode in air;* diameter of high voltage points: 50 um - 200 um; distance to LV electrode: 25 mm; test voltage: 16 kVeff.
6. *Multiple corona discharges at the LV electrode in air;* diameter of low voltage points: 50 um - 200 um; distance to HV electrode: 15 mm; test voltage: 5.6 kVeff.
7. *Surface discharges between two dielectric surface;* test voltage = 29kVeff;
8. *Contact noise*; Imperfect metal-to metal joint in the HV electrode; test voltage: 2.2 kVeff.
9. *Floating object;* Badly earthed metallic component near HV circuit; ungrounded metallic plate at 500 mm distance from HV terminal of a discharge free test object; test voltage 28 kVeff.
10. *PD on external dielectric;* Two touching insulated conductors; surfaces PD between two touching 6/10 kV PE cables; test voltage 13 kVeff.
11. *LV electrode-bounded cavity;* dielectric: polyethylene; Flat cavity between PE/metal; 16mm x 0.4mm; test voltage: 11 kVeff; average field strength: 2.43 kV/mm.
12. *Dielectric-bounded flat cavity;* dielectric: polyethylene; Flat cavity in PE; 16mm x 0.4mm; test voltage: 11 kVeff; average field strength: 2.35 kV/mm.
13. *Dielectric-bounded cavities;* dielectric: polyethylene; Flat cavities in PE; 5 cavities of 4mm x .4mm; test voltage 12 kVeff; average field strength: 2.7 kV/mm.

14. *LV electrode-bounded cavities;* dielectric: polyethylene; Flat cavities between PE/metal; 5 cavities of 4mm x .4mm; test voltage: 12 kVeff; average field strength: 2.9 kV/mm.
15. *Fissure PD between PE-foils;* Fissure between two PE layers HV electrode: .05mm aluminum foil; PD due to high tangential field- strength in the fissure at the end of HV electrode; PD occur between two 0.1 mm PE foils; test voltage = 12 kVeff
16. *Background noise*
17. *No Partial Discharges*

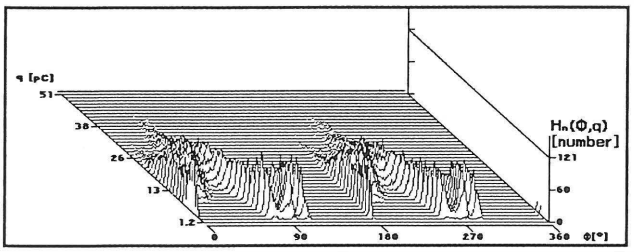

Figure 6 The 3D plot as observed on 23 kV epoxy insulator. The origin of PD reveals air pockets around ceramic core.

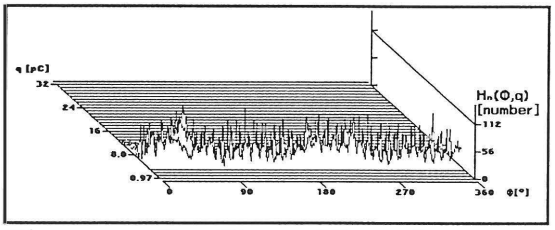

Figure 7 The 3D plot as observed on 10nF/220 kV mixed insulation capacitor. The origin of PD reveals to a bad solder joint between capacitor packages inside the capacitor.

Each of these defects is represented by 282 *fingerprints* as obtained on different samples and stored in the *device* 'ARTIFICIAL DEFECTS', each as a separate *problem*. In the following this collection of known *fingerprints* will be used to recognize unknown discharges in two HV constructions. In figures 6 and 7 examples of 3 dimensional relationship between discharge magnitude, PD intensity and the phase angle $H_n(\phi,q)$ distribution are presented. As shown in these figures different insulation defects in industrial objects are characterized by typical differences in the landscape of such 3 dimensional figures. It confirms the opinion that these $H_n(\phi,q)$ distributions as mentioned here might be very useful to analyse the discharge processes in actual HV equipment.

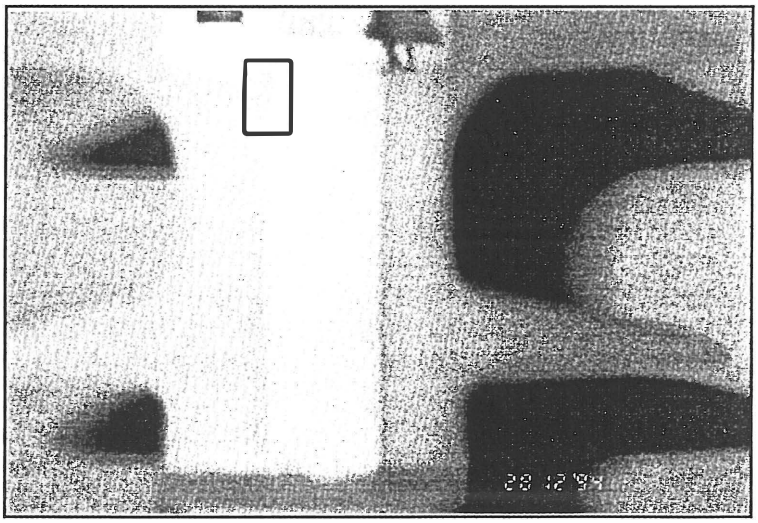

Figure 8 Photograph of the cross section of the 23 kV epoxy insulator showing location of the air pockets.

4.1 Cavity Discharges in Epoxy Resin Insulator

In a 23 kV insulator the origin of discharges was related to air pockets around the ceramic core of the insulator which remained after casting, see figure 8. In figure 9 the phase-position quantities Hqmax(ϕ), Hqn(ϕ) and Hn(ϕ) as obtained during 2 minutes at 23 kV are shown. Furthermore in figures 10 and 11 the *fingerprint* and the result of recognition are shown.

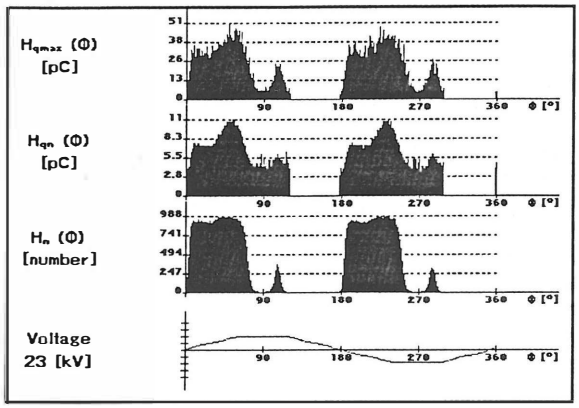

Figure 9 The phase position distributions as observed on 23 kV epoxy insulator.

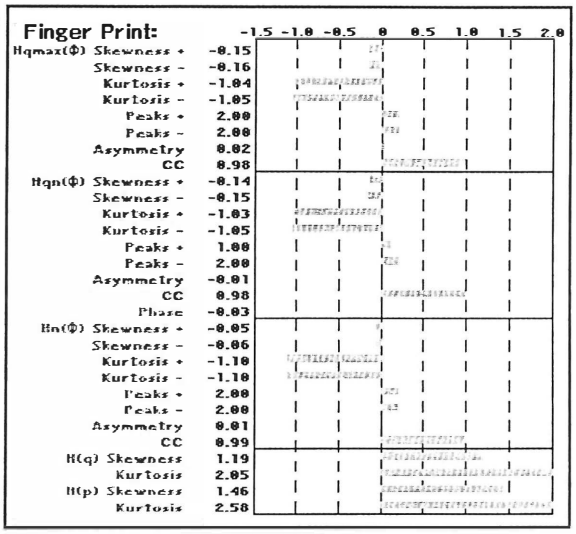

Figure 10 The fingerprint as processed for the measuring data in figure 9.

The comparison to the 'ARTIFICIAL DEFECTS' recognizes clearly internal discharges (93%) cavities dielectric bounded; the resemblance to other defects is low.

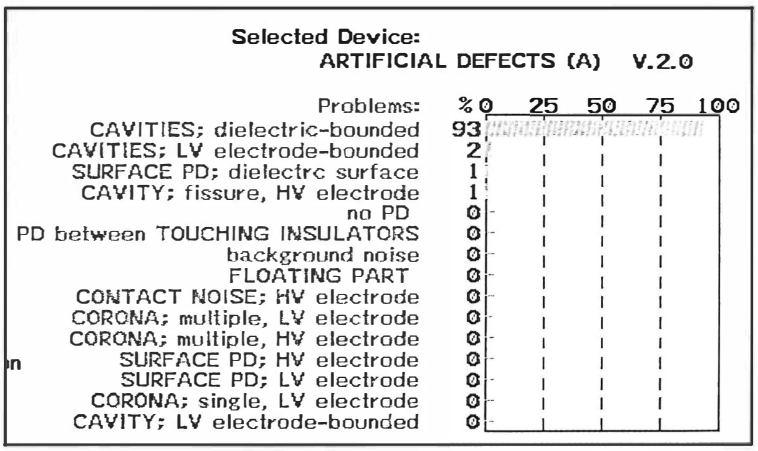

Figure 11 Result of statistical recognition of measuring data from figures 9 and 10 using TEAS 570 PD data bank Artificial Defects .

4.2 Contact Noise Discharge in Mixed Insulation Capacitor

A 10nF/200 kV capacitor showed discharges which are due to a bad solder joint between capacitor packages inside the capacitor, see figure 12.

This object was tested during 2 minutes at 160 kV test voltage. In figures 13, 14 and 15 the phase position quantities Hqmax(ϕ), Hqn(ϕ) and Hn(ϕ) as well as the *fingerprint* and the result of comparison to 'ARTIFICIAL DEFECTS' are shown. It follows from figure 15 that the contact noise (100%) was clearly recognized and the floating part (10%) to a lesser extend. Also there is no

resemblance to other defects.

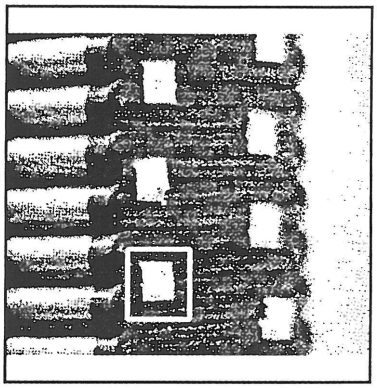

Figure 12 Photograph of capacitor packages showing a solder joint.

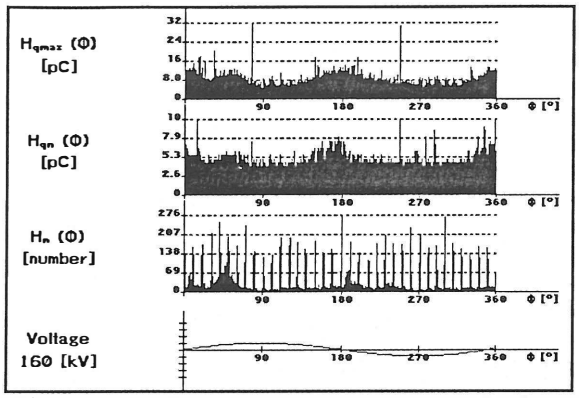

Figure 13 The phase position distributions as observed on 10nF capacitor.

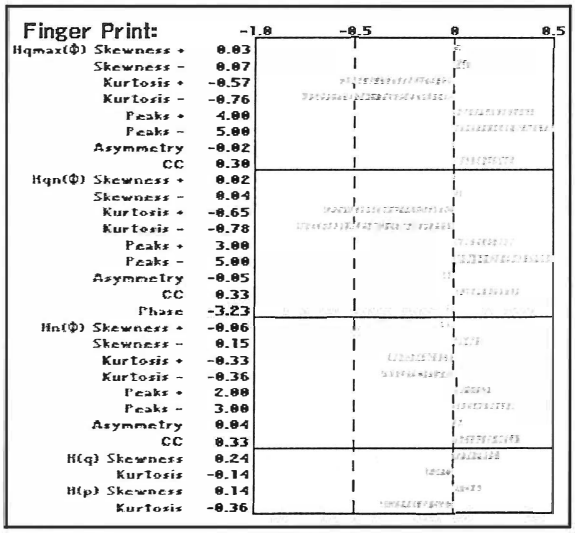

Figure 14 The fingerprint as processed for the measuring data in figure 13.

Figure 15 Result of statistical recognition of measuring data from figures 13 and 14 using TEAS 570 PD data bank Artificial Defects .

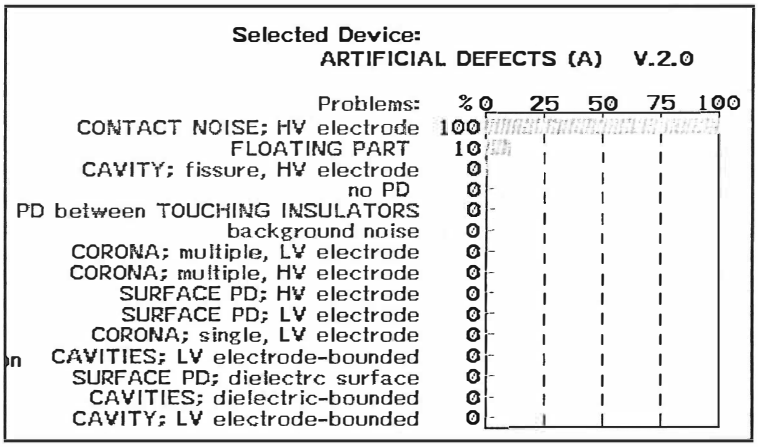

5. PD Source Recognition Using 'INDUSTRIAL PROBLEMS'

In the previous section the usefulness of the *fingerprint* method is shown by the analysis of two industrial defects and their recognition using the **device** *'ARTIFICIAL DEFECTS'*.
Of course, the similarity between an artificial defect (two-electrode models) and its industrial counterpart may be very small in praxis.
Therefore it is equally important to develop a second type of *PD data bank* which shall contain HV constructions and industrial problems.
It's known that with regard to a particular HV construction a number of discharge causes can occur, which are specific for this component.
With the *fingerprints* of these discharges a catalog of possible *problems* can be made. Such a collection is of importance when in the future similar situations occur.
In the following practical examples are presented of a **device** called *'350/400kV Transformers'*.
This device was developed after the analysis of discharges in different: 350 kV and 400 kV transformer test sets. Moreover, the defects as mentioned in this section could actually be found and could be repaired. In particular five different discharge sources were studied and their *fingerprints* were used to define the industrial problems, see figure 16.

1. *Bushing discharges (350 kV transformer),*
2. *Coil discharges (350 kV transformer),*
3. *Foreign part discharges (400 kV transformer),*
4. *Surface corona discharges (400 kV transformer),*
5. *Oil discharges (400 kV transformer),*

In figure 17 and 18 examples of 3 dimensional distribution Hn(ϕ,q) as observed for two industrial problems are shown. Similar to results in figure 6 and 7 the same conclusions can be drawn from these diagrams: very atractive for the eye.

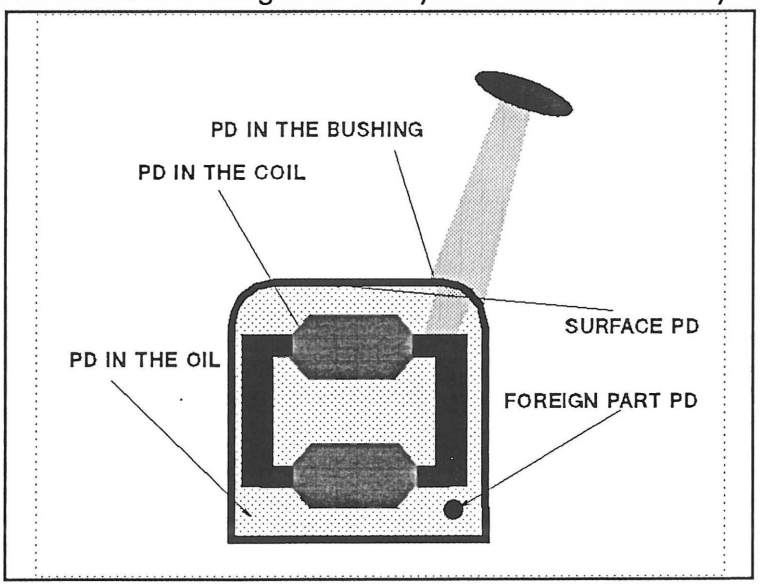

Figure 16 Cross section of a transformer test set showing industrial defects.

First of all these five groups, each represented by at least 30 *fingerprints* were mutually compared in order to see whether and in what measure they could be

distinguished from each other.

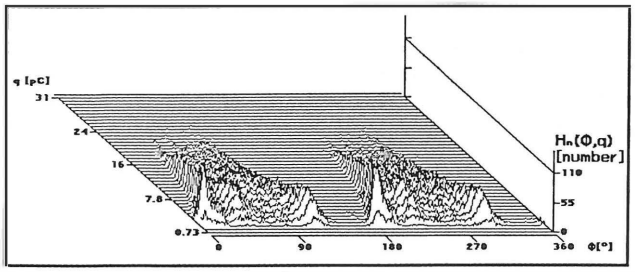

Figure 17 The 3D plot as observed on bushing discharges in a 350 kV test transformer.

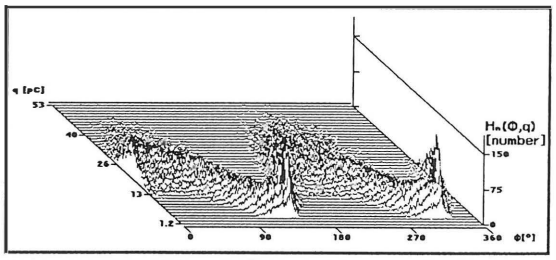

Figure 18 The 3D plot as observed on coil discharges in 350 kV test transformer.

This was done by calculating the classification if one of the five *fingerprints* is compared with either itself (self-recognition) or with the other four. This proved to be quite successful: self-recognition was 98% to 100%, whereas the clas sification fell below 40% when the other defects were entered.
This proves that sufficient distinction between these five 'industrial problems' exists.

5.1 Bushing Discharges in 350 kV Test Transformer

The 350 kV transformer test set showed discharges caused by a bad connection of the bushing inside the transformer tank.
Four tests of 2 minutes were carried out at 350 kV test voltage. The collection of 120 *fingerprints* was used to define the 'industrial problem': *Bushing discharges (350 kV Transformer)*. In figures 19, 20 and 21 examples of the phase-position quantities, their *fingerprint* and the results of the recognition are shown. It follows from the classification that this type of defect: 'Bushing discharges' is clearly recognized: 100%. The resemblance to other defects as measured in both types of the transformer is low.

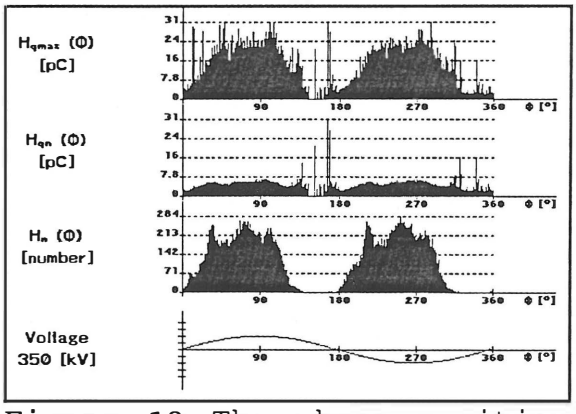

Figure 19 The phase position distributions as observed on bushing discharges in 350 kV test transformer.

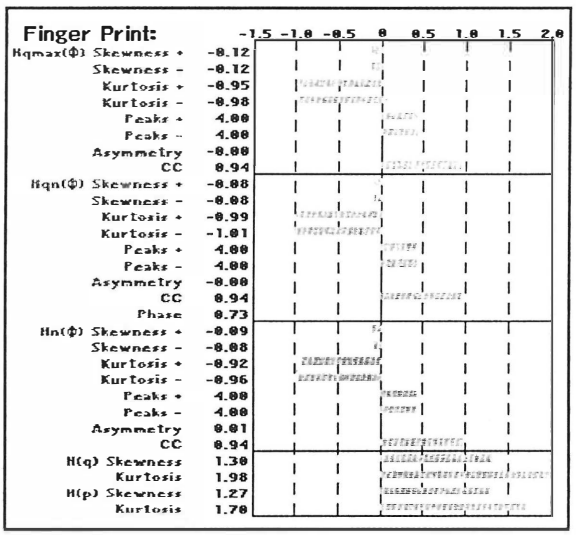

Figure 20 The fingerprint as processed for the measuring data in figure 19.

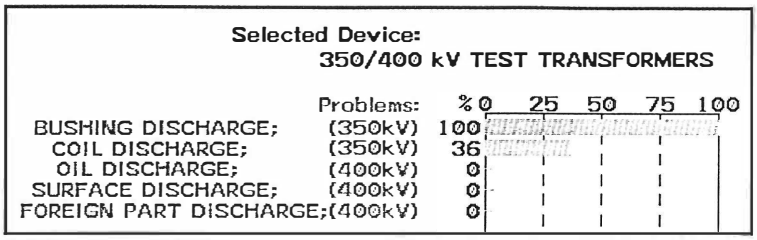

Figure 21 Result of statistical recognition of measuring data from figures 19 and 20 using TEAS 570 PD data bank Artificial Defects .

5.2 Coil Discharges in 350 kV Test Transformer

Internal discharges were found inside a coil of a 350 kV transformer test set. Nine tests of 5 minutes were performed at 200 kV test voltage.

The collection of 270 *fingerprints* were used to define the 'industrial problem': *Coil discharges (350 kV Transformer)*. In figures 22, 23 and 24 examples of the phase-position quantities, their *fingerprint* and the result of the recognition are shown.

It follows from the classification diagram that this type of defect: 'Coil discharges' is 100% recognized. There is no resemblance to other defects.

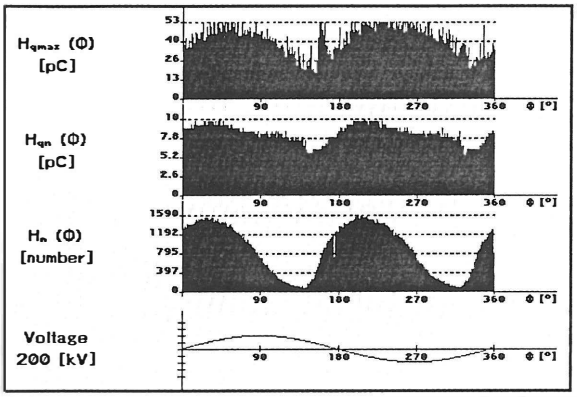

Figure 22 The phase position distributions as observed on coil discharges in 350 kV test transformer.

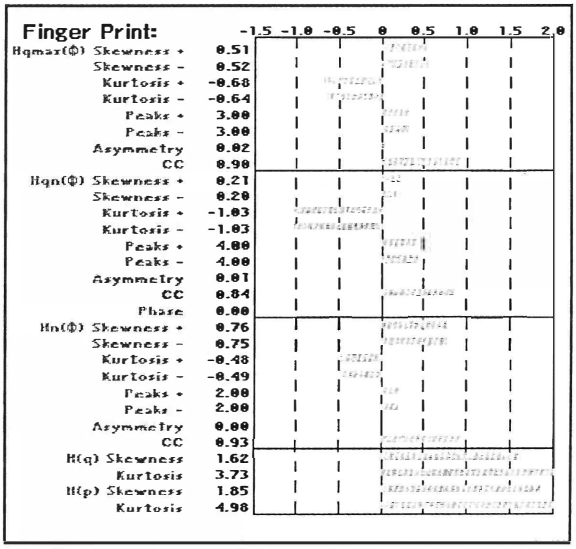

Figure 23 The fingerprint as processed for the measuring data in figure 22.

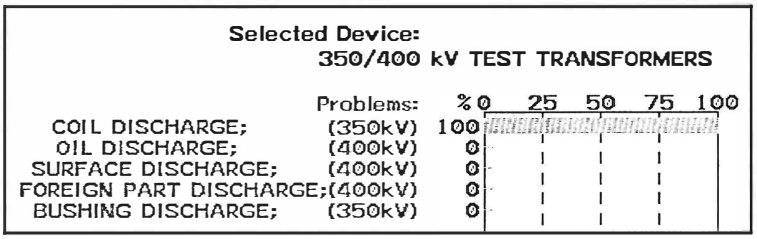

Figure 24 Result of statistical recognition of measuring data from figures 22 and 23 using TEAS 570 PD data bank Artificial Defects .

6. Insulation Degradation Monitoring Using 'AGING STAGES'

In previous sections the use of *PD data bank* technique to recognize different discharging faults was shown. Equally important to such recognition is also the determination of degradation of discharging dielectric. Therefore using this

method in long term test internal discharges in epoxy insulation of a 30/50 kV current transformer will be analyzed. A 30/50 kV current transformer with epoxy insulation was continuously aged for 1361 hours at 52 kV. Discharges occurred from the very beginning, possibly located in multiple cracks in the epoxy near the conductor [4], see figure 25.

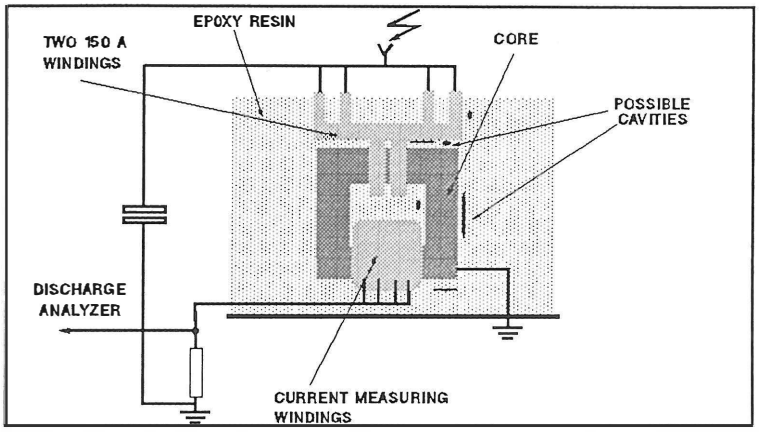

Figure 25 Cross-section of the 2x150A/5A 30/50 kv current transformer with indication of possible discharge sources.

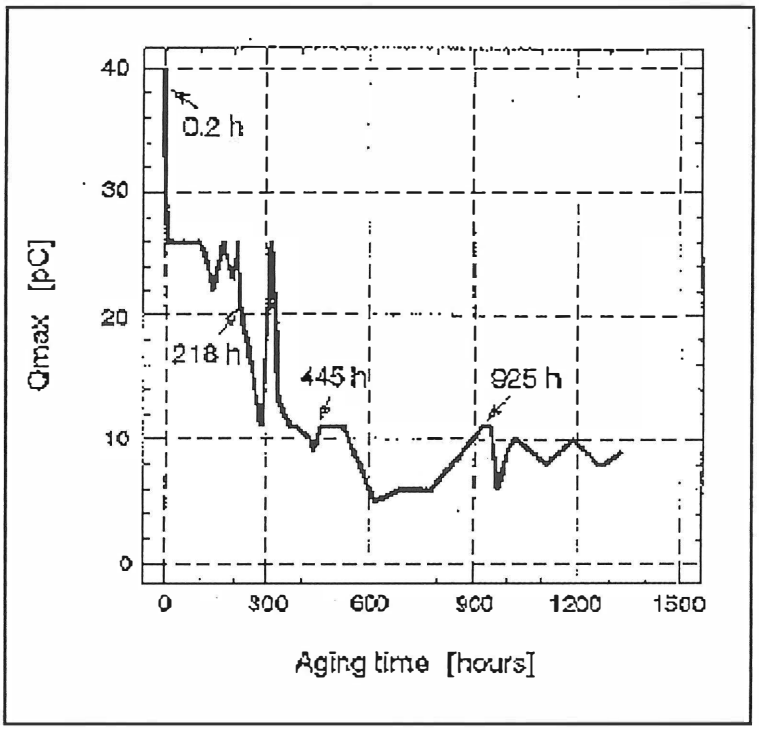

Figure 26 The time behaviour of the maximum discharge magnitude as observed during 1361 hrs aging at 52 kV of epoxy resin current transformer.

During aging time of 1361 hours in regular intervals discharge detection was carried out where one such PD measurement was preformed for 10 minutes. To represent in proper way the development of the discharge process altogether 54 measurements were carried out during 1361 hours test. In figure 26 the time behaviour of the maximum discharge magnitude is shown.
It can be seen from this figure that after 300 hours aging significant decrease in the discharge magnitude has been observed, and after this change no remarkable variation are registered.

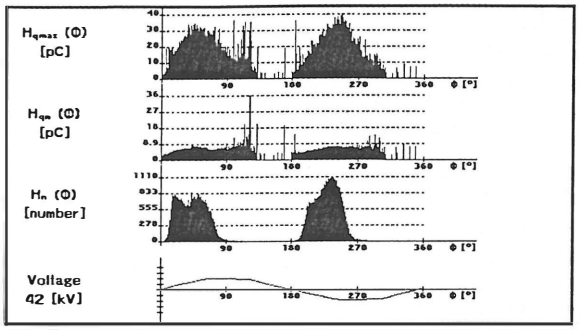

Figure 27 Phase-position distributions as observed after 10 minutes aging of 30/50 kV epoxy resin current transformer.

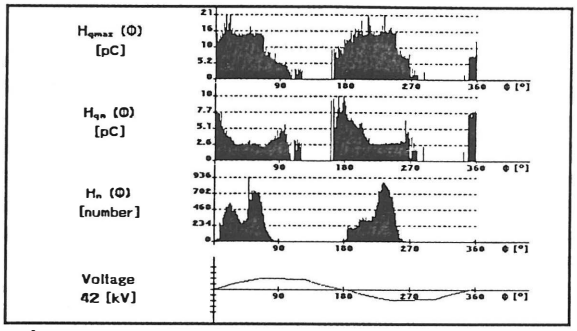

Figure 28 Phase-position distributions as observed after 218 hrs aging of 30/50 kV epoxy resin current transformer.

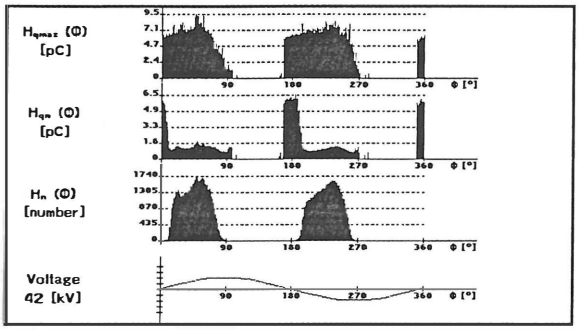

Figure 29 Phase-position distributions as observed after 445 hrs aging of 30/50 kV epoxy resin current transformer.

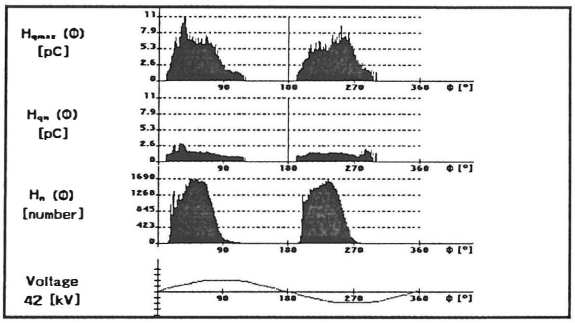

Figure 30 Phase-position distributions as observed after 925 hrs aging of 30/50 kV epoxy resin current transformer.

Parallel to each measurement of the discharge magnitude also phase-resolved detection and analysis was preformed. In figures 27-30 typical phase-position distributions as observed at different moments during the test are shown: 10 minutes, 218 hours, 445 hours and 925 hours. It follows from these figures that not only the decrease in the discharge magnitude occurs but also characteristic changes in the shape of all three phase-position quantities are visible. All these distributions as observed at different points in the aging time are processed using statistical operators.

These 54 *fingerprints* were further analyzed in order to see whether and in what measure they could be distinguished from each other. As a result four consecutive categories or groups called further in the text stages were created and tested.

The first group appears between 0 and 100 hours, the second between 100 hours and 330 hours, the third between 330 hours and 530 hours and the fourth from 530 hours till the end of the test. Based on this clustering all *fingerprints* were combined into consecutive groups called *stage 1, stage 2, stage 3* and *stage 4*. Based on these groups new data bank 'AGING STAGES OF 50 kV CT' was developed. Similar to 17 problems of the data bank 'ARTIFICIAL DEFECTS' this new data bank contains 4 *problems*: *stage 1, stage 2, stage 3* and *stage 4*.

Statistical evaluation of mutual comparison of all *fingerprints* was made in order to see whether and in what measure they could be distinguished from each other. In table 1 results of this classification are shown. In particular individual *fingerprints* were compared with its own group and with the other three. To evaluate results of classifications, the following outputs were used.

1. **CORRECT RECOGNITION**: the *fingerprint* is correctly classified. The following rules were applied: the classification must be larger than 30% and the difference between the first and second classification must be at least 30%.
2. **SEMI-CORRECT RECOGNITION**: the *fingerprint* is assigned to several categories including the correct one. The difference between the first and second classification is less than 30% and the first classification larger than 30%.
3. **NO RECOGNITION**: the *fingerprint* is not assigned to any of the known categories. We propose that the first classification should be less than 30%.
4. **INCORRECT RECOGNITION**: the *fingerprint* is incorrectly classified.

STAGES	CORRECT RECOGNITION	SEMI-CORRECT RECOGNITION	NO RECOGNITION	INCORRECT RECOGNITION
1	66%	34%	—	—
2	100%	—	—	—
3	91%	—	9%	—
4	78%	—	22%	—

Table 1 *Results of classifications of four aging stages for a 30/50 kV current transformer.*

This proves that sufficient distinction between the four stages exists. In none of these cases mis-classification occurred, that is: in neither case the wrong stage of discharge was indicated.
In figures 31-34 results of recognition using this new data bank are shown. The *fingerprints* as processed for 10 minutes, 218 hours, 445 hours and 925 hours aging are compared to the data bank 'AGING STAGES OF 50 kV CT'. It follows, that the individual results which were obtained during the course of 1361 hours test can clearly be classified to one of the consecutive stages.

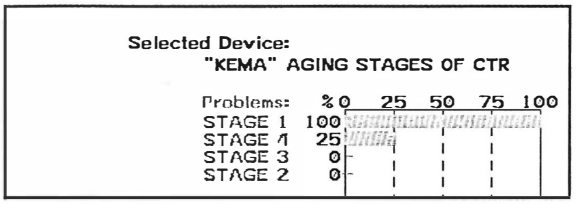

Figure 31 Recognition by PD data bank AGING STAGES OF 50 kV CT of fingerprint as observed after 10 minutes aging.

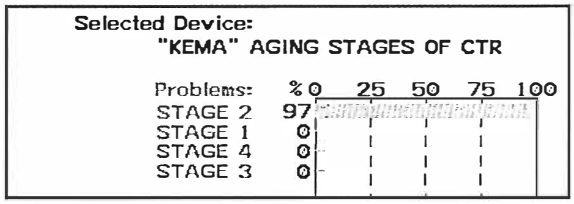

Figure 32 Recognition by PD data bank AGING STAGES OF 50 kV CT of fingerprint as observed after 218 hrs aging.

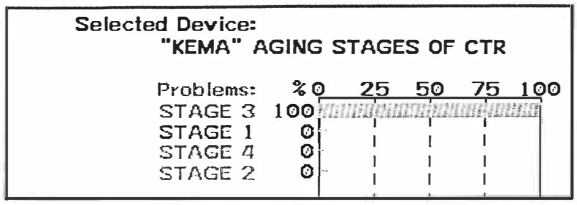

Figure 33 Recognition by PD data bank AGING STAGES OF 50 kV CT of fingerprint as observed after 445 hrs aging.

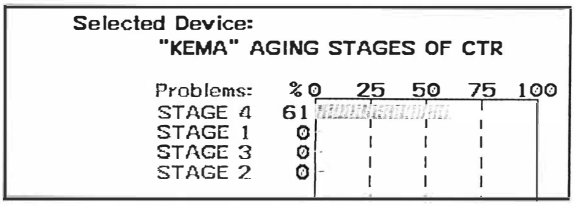

Figure 34 Recognition by PD data bank AGING STAGES OF 50 kV CT of fingerprint as observed after 925 hrs aging.

It follows from these observations that conventional detection of PD is well able to indicate different stages of insulation aging. Of course these stages need not necessarily be identical to the three stages as mentioned in [4], but they show that aging stages occur in actual HV equipment and can be recognized as such, see figure 35.

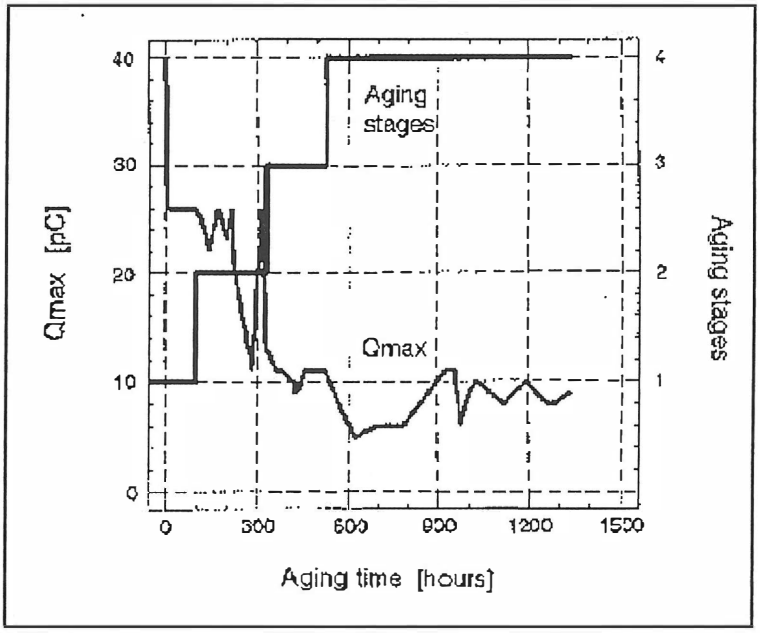

Figure 35 The time behaviour of the maximum discharge magnitude as shown in figure 26 extended by stages which were determined during 1361 hrs aging at 52 kV of epoxy resin current transformer.

Acknowledgements: The measuring data as presented in the section 6 are result of scientific cooperation between Department of Electrical Research and Information Technology of N.V. KEMA, Arnhem, The Netherlands and High Voltage Laboratory of Delft University of Technology, The Netherlands

7. Conclusions

This systematic attempt to apply **the *fingerprint* technique** to develop a *PD data bank* of **full scale HV constructions** is encouraging. The results obtained are summarized as follows.

1. It has been shown that the use of conventional detection combined with statistical analysing techniques as incorporated in TEAS opens the possibility to recognize different discharge sources and to monitor the changes in the

insulation.

2. The conventional discharge detection (including a statistical analyzer TEAS 570) is well suited for recognizing the stages of deterioration of dielectrics by discharges. Without any question, systematic tests till breakdown are requested and are under way. Moreover, the ability to test more than one discharge source in the same HV apparatus has to be studied.

3. The proposed **device/problem structure** for the storage of *fingerprints* in a ***PD data bank*** is straightforward and can very efficiently be used.

4. Using physical models of discharges their presence in complete HV constructions can be proven. In this way the applicability of results as obtained from physical models of discharges for the evaluation of the full scala HV constructions is possible.

5. Using the *fingerprint* technique the properties of several 'industrial defects' of full scale HV constructions can be classified and this information can be useful to recognized defects and to take the measures to make repairs.

6. Using the presented method the final goal to recognize defects in actual industrial objects becomes more realistic. Needless to say, this task requires many years of practical experience of engineers in the test departments of the manufacturers, the testing institutions and the users.

7. References

[1] E. Gulski, Computer-aided Measurement of PD in HV Equipment, IEEE Trans. on Elec. Insulation, Vol 28, No.6, 1993

[2] E. Gulski, P. Seitz, Computer-Aided Registration and Analysis of PD in HV Equipment, in Proceedings of 8th Inter. Symp. on High Voltage Engineering, Yokohama 1993, Japan

[3] F.H. Kreuger, E. Gulski, A. Krivda, Classification of PD, IEEE Trans. on Elec. Insulation, Vol 28, No.6, 1993

[4] F.H. Kreuger, P.H.F Morshuis, E. Gulski, Evaluation of Discharge Damage By Fast Transient Detection and Statistical Analysis, paper 15-106, CIGRE Session, 1994, Paris.

[5] E. Gulski, Computer-Aided Recognition of PD Using Statistical Tools, Delft University Press, 1991